Shear-thinning drop formation

M. R. Davidson   J. J. Cooper-White   V. Tirtaatmadja[*]

Abstract

A volume-of-fluid numerical method is used to predict the dynamics of drop formation from a nozzle with a circular exit, directed vertically downwards in air, when the drop fluid is shear-thinning. The validity of the numerical calculation is first confirmed for a Newtonian fluid by comparison with experimental measurements. For the cases considered, predictions for a shear-thinning drop fluid result in more rapid pinch-off and a smaller final neck length consistent with a related study of liquid bridges.

Contents

---

[*]Department of Chemical and Biomolecular Engineering, The University of Melbourne, Parkville, Victoria 3010, Australia. mailto:m.davidson@unimelb.edu.au

1 Introduction

The growth and detachment of drops from a nozzle is important in many circumstances, ranging widely from the industrial (for example, ink-jet printing, liquid-liquid extraction, spraying, biological assays) to the domestic (for example, a dripping tap). For drop formation from a nozzle under the influence of gravity, the liquid flow rate is low and the pendant drop grows slowly at first, characterised by a quasi-static balance between gravity and interfacial tension. However, once the drop volume reaches a critical value, force equilibrium is lost and the evolution of the drop rapidly accelerates leading to necking and break-up (pinch-off) of the pendant drop.

The evolution of a pendant drop has been a topic of investigation for more than a century. Following the publication of high definition photographs, showing the dynamics close to pinch-off [9], research activity on this topic has expanded rapidly, including more in-depth experimental observations [7, 4]. A detailed review of recent fluid dynamic research on interfacial break-up phenomena for dripping nozzles, jets, liquid bridges and other related problems is given by Eggers [5]. More recent summaries concerning pendant drops have been given by Wilkes et al. [12] and Cooper-White et al. [4].

The first numerical studies were based on one-dimensional slender thread approximations (for a detailed discussion and references, see [5]). Numerical studies which dispense with the one-dimensional approximation include

boundary integral solutions of potential flow [11] and Stokes flow [14], and finite element [12, 2] and volume-of-fluid [6, 15] solutions of the full Navier-Stokes equations.

Thus far, most studies of drop formation and pinch-off concern Newtonian liquids. However, in many practical circumstances (for example, ink-jet printing, biological fluids), the drop fluid is non-Newtonian in character. The evolution of a pendant drop of visco-elastic fluid has been studied experimentally by Amarouchene et al. [1] and more comprehensively by Cooper-White et al. [4]. Yildirim and Basaran [13] used a finite element numerical method to examine the deformation and breakup of Newtonian and shear-thinning liquid bridges contained between two disks, a problem closely related to that of the pendant drop. However, there appears to be no published numerical study of the evolution of a pendant drop of non-Newtonian liquid. The aim of the present work is to demonstrate the use of a volume-of-fluid (VOF) numerical method to predict the growth and eventual pinch-off of a pendant drop of shear-thinning liquid.

2   Formulation

The growth of a pendant drop into ambient air from a nozzle of internal diameter $2a$ and external diameter $4a$ is considered (Figure 1). The mean inflow velocity of the liquid entering the drop from the nozzle is denoted by $\bar{V}$. The liquid is assumed to wet the nozzle so that the liquid-air interface is attached at the outer diameter of the nozzle. Axi-symmetric evolution of the drop is investigated from a stable initial state (Figure 1(i)).

In terms of dimensionless velocity, length and time, scaled according to $\bar{V}$,
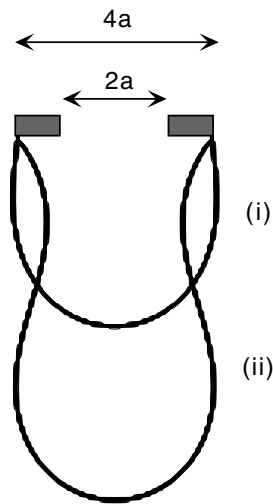
FIGURE 1: Schematic showing: (i) the initial drop shape; and (ii) the drop shape at a later time. The shaded parts indicate the annular solid section between the inner and outer radii of the nozzle exit.

a and $a/\bar{V}$, respectively, the equations of motion for a VOF calculation are

$$\frac{\partial C}{\partial t} + \nabla \cdot (\boldsymbol{U}C) = 0 \,, \tag{1}$$

$$\frac{\partial \rho \boldsymbol{U}}{\partial t} + \nabla \cdot (\rho \boldsymbol{U}\boldsymbol{U}) = -\nabla P + \frac{1}{\mathrm{Fr}}\rho \hat{\boldsymbol{g}} + \frac{1}{\mathrm{We}}\boldsymbol{F_S} + \frac{1}{\mathrm{Re}}\nabla \cdot \boldsymbol{\tau} \,, \tag{2}$$

$$\nabla \cdot \boldsymbol{U} = 0 \,, \tag{3}$$

$$\rho = \rho_1 C + \rho_2 (1 - C) \,, \tag{4}$$

where C is a fractional volume function, P denotes pressure, $\boldsymbol{\tau}$ is the viscous stress tensor, $\hat{\boldsymbol{g}}$ is a unit vector pointing in the direction of gravity and $\boldsymbol{F_S}$ is the surface force arising from interfacial effects. The subscripts 1 and 2 denote values for the liquid (drop) phase and air phase, respectively. The fractional volume function C is advected with the local velocity $\boldsymbol{U}$. The above equations correspond to the flow of a mixture with variable properties (density and viscosity), combined with advection of the volume fraction. The mixture takes the properties of the liquid within the drop and those of air within the surroundings, with a volume fraction weighted average in computational cells containing the interface. The interface position is determined implicitly at any time by consideration of the volume fraction distribution.

The Carreau model of a shear-thinning fluid is used here for the drop fluid. This model gives an expression for the liquid viscosity (μ_1) which varies smoothly from its value at zero shear rate (μ_{10}) to a lower value at very large shear rate ($\mu_{1\infty}$). If we use μ_{10} as the viscosity scale for the non-dimensional problem, then the dimensionless Carreau viscosity ($\eta = \mu_1/\mu_{10}$) is

$$\frac{\eta - \eta_\infty}{1 - \eta_\infty} = \left(1 + (\lambda \dot{\gamma})^2\right)^{\frac{1}{2}(n-1)} \,, \tag{5}$$

where $\dot{\gamma}$ is the dimensionless shear rate, λ is a dimensionless time constant, $\eta_\infty = \mu_{1\infty}/\mu_{10}$ and $n < 1$. Note that $n = 1$ corresponds to a Newtonian fluid. The shear rate is

$$\dot{\gamma} = \sqrt{\nabla \boldsymbol{U} : (\nabla \boldsymbol{U} + (\nabla \boldsymbol{U})^T)} \,, \tag{6}$$

which derives from its expression in terms of the second invariant of the rate of strain tensor [3].

The dimensionless parameters in Equations (1–3) are the Froude, Weber and Reynolds numbers respectively:

$$\mathrm{Fr} = \frac{\bar{V}^2}{ga}, \quad \mathrm{We} = \frac{\rho_1 \bar{V}^2 a}{\sigma}, \quad \mathrm{Re} = \frac{\rho_1 \bar{V} a}{\mu_{10}}. \tag{7}$$

Here, σ is the coefficient of surface tension between the liquid and the air, and g is the acceleration due to gravity.

The computational domain containing the drop is taken to be a cylindrical region about the axis of symmetry, with a top boundary which is impervious except for an inlet disc $r < a$ coinciding with the nozzle exit. As in [6], the vertical (inflow) velocity profile at the inlet is taken to be a linear function of radius, with the same linear velocity profile at the bottom of the computational domain to conserve the total volume of fluid therein. The results are not sensitive to the choice of velocity profile. Zero normal gradients in C are set at the boundaries of the computational domain except at the inlet where $C = 1$. Free slip velocity conditions are taken at the radial boundary of the domain; however the choice of slip or no-slip there is irrelevant since the fluid at this boundary is entirely air, the dynamics of which is unimportant.

The stable drop shape used as an initial condition was determined in a separate flow calculation with zero inflow at the nozzle, beginning with a drop shape of known volume (in dimensionless terms, we choose $40\pi/3$, corresponding to a cylinder of radius 2 and height 2, capped at its base by a hemisphere of radius 2). This pre-calculation of drop shape readjustment was continued until a stationary configuration was achieved, representing an equilibrium between gravitational and surface tension forces.

The VOF algorithm of Rudman [10] was adapted to solve Equations (1–3) for shear-thinning fluids. The semi-implicit time stepping procedure of Li and Renardy [8] was incorporated to remove the diffusion time step limitation

in the explicit Rudman algorithm; this is essential for calculating very low Reynolds number flows. Axi-symmetric flow calculations were performed in cylindrical polar coordinates on the symmetric half of a computational domain having radius $4a$ (that is, twice the outer radius of the nozzle) and height $16a$ ($24a$, $32a$). A 64×256 (64×384, 64×512) staggered grid is used. The longer computational domains become necessary when the initial liquid viscosity is increased. Finally, the radial velocity in the top row of cells for $r > a$ was set to zero to numerically pin the contact line at the edge of the nozzle.

3   Results and Discussion

To test the validity of the numerical calculation, predictions of drop shape are compared with corresponding photographic images of a Newtonian drop in an experiment for which $\rho_1 = 1126 \, \text{kg/m}^3$, $\mu_1 = 0.006 \, \text{Pa} \, s$, $\sigma = 0.07 \, \text{N/m}$. The nozzle inner radius $a = 1 \, \text{mm}$ and the volumetric flow rate of liquid is $74 \, \text{ml/hr}$, giving a mean inflow velocity $\bar{V} = 6.54 \, \text{mm/s}$. The corresponding values of the dimensionless groups are Re $= 1.25$, We $= 0.000687$, Fr $= 0.00437$. We also set the air/liquid ratios $\rho_2/\rho_1 = 0.001$ and $\mu_2/\mu_{10} = 0.003$. Two other commonly used dimensionless groups are the Ohnesorge number Oh $= \text{We}^{\frac{1}{2}}/\text{Re} = \mu_{10}/(\rho_1 \sigma a)^{\frac{1}{2}}$ and the Bond number Bo $= \text{We/Fr} = \rho_1 a^2 g/\sigma$. For the experiment considered Oh $= 0.021$ and Bo $= 0.157$.

Figure 2 shows the comparison between predicted and observed drop shapes for the above-mentioned experiment. To synchronise the predicted and photographic images, we have assumed that the moment of pinch-off occurs physically when the calculated minimum dimensionless thickness of the neck is 0.01 which is the approximate resolution of the grid. The VOF numerical method is not sufficiently accurate to precisely resolve the moment of pinch-off; however, Figure 2 shows that the overall detail of the drop shape (including neck and the satellite drop formation) are closely reproduced. In-
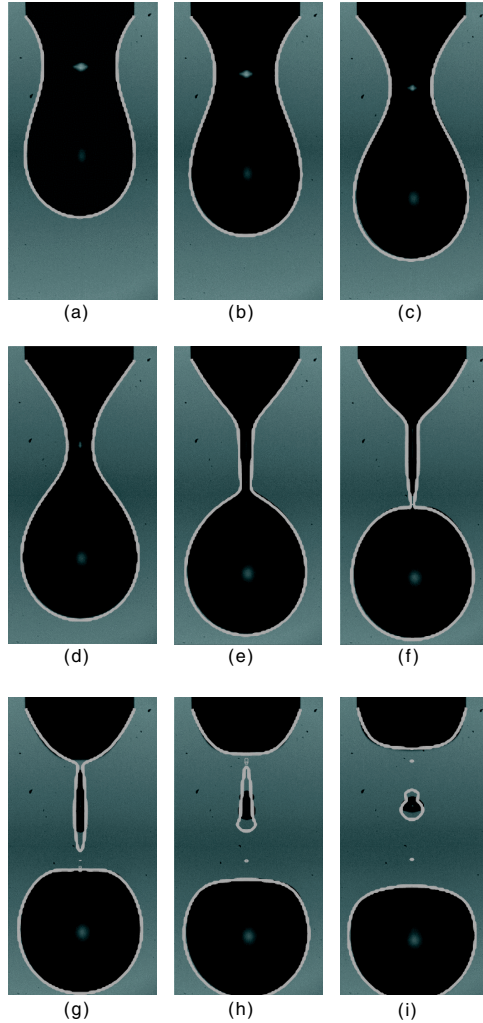
FIGURE 2: Comparison between predicted drop shapes (white outlines) and corresponding photographic images for a Newtonian drop. The times in the sequence $(a - i)$ are -30, -20, -10, -5, -1, 0, 1, 2, 3 milliseconds, respectively, relative to the moment of pinch-off.
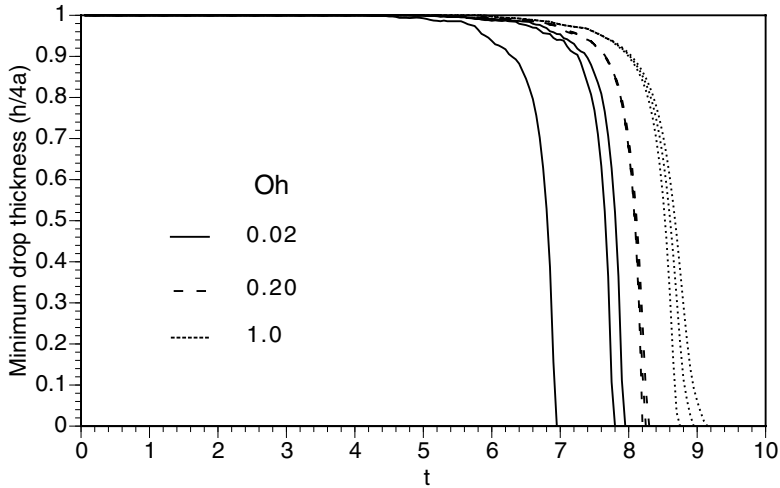
FIGURE 3: Minimum drop thickness, scaled with the outer nozzle diameter, for Newtonian ($\eta_\infty = 1.0$) and shear-thinning liquids ($\eta_\infty = 0.2, 0.6$) for different values of Oh, when We $= 0.000687$, Fr $= 0.00437$. Other (shear-thinning) parameters are $\lambda = 1$, $n = 0.2$. For each Oh value, the curves shift to the right with increasing η_∞.

creasing the mesh size density from 64×256 to 96×384 resulted in negligible changes to the predicted drop shapes.

The effect of reducing the zero shear viscosity (reducing Oh) or η_∞ (the infinite shear/zero shear viscosity ratio) on the minimum neck width is shown in Figure 3 as a function of time. The values of We and Fr in these and all subsequent calculations are the same as in the experiment. When η_∞ is less than 1.0 ($\eta_\infty = 1$ is the Newtonian case), the liquid viscosity decreases from its initial (zero shear) value as the drop evolves. Decreasing either Oh or η_∞, keeping the other fixed, results in more rapid thinning of the neck (although the effect is small for Oh $= 0.2$). This occurs because the normal viscous stresses act to reduce the liquid pressure at the neck where it is a

maximum, so that reducing the viscosity increases that pressure which, in turn, increases the drainage of the neck liquid. This effect of viscosity has been noted in relation to Newtonian drops [12] and liquid bridges [13]. The larger effect of shear thinning when Oh = 0.02 may seem surprising since one would expect the effect to become small when Oh is small (that is, when the effect of viscosity is small compared with that of surface tension) [13]. However further work (not presented here) shows that the effect of shear thinning reduces for Oh < 0.02 and becomes negligible for Oh = 0.0002. Calculations at these lower Oh (lower viscosity) values require the inclusion of the nozzle region in the calculation because of penetration by an increased upward flow out of the neck [12].

Figure 4 shows the predicted evolution of drop shapes and viscosity maps for Oh = 0.2. The more rapid approach to pinch-off as η_∞ decreases is obvious, but the differences only occur over a small time interval, consistent with Figure 3. In each case, pinch-off is found to occur from the bottom of the neck. Yildirim et al. [13] found that pinch-off of a liquid bridge could occur from the bottom or the top of the neck, depending on the stretching speed. The viscosity maps in Figure 4 illustrate the reduction in viscosity as pinch-off of a shear-thinning fluid is approached and velocity gradients increase, especially in the neck region. Yildirim et al. [13] found a qualitatively similar outcome for the viscosity of shear-thinning liquid bridges.

The trends for Oh = 1.0 (higher zero shear viscosity) are not shown, but are similar to those in Figure 4. Overall, pinch off occurs later than for Oh = 0.2 (as discussed for Figure 3) and over a longer time interval. The neck filament becomes longer than for the lower viscosity case for the same reason that pinch-off is delayed [12]. Also for the same reason, pinch-off is approached more rapidly (as for Figure 4), and the final neck length becomes smaller, as η_∞ is reduced.
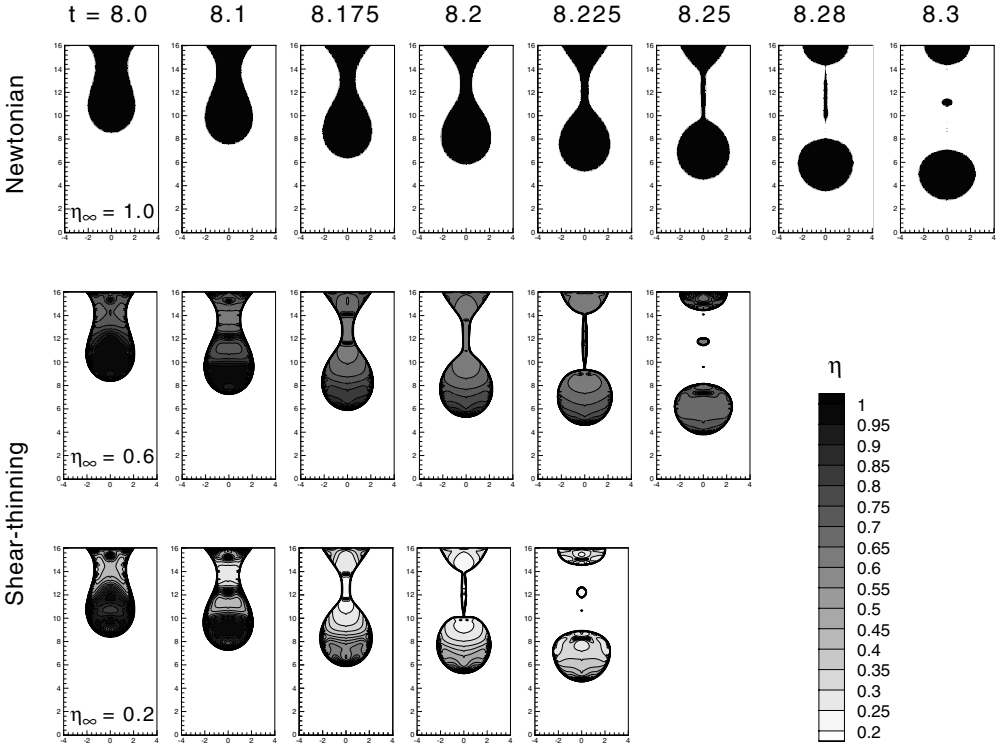
FIGURE 4: Predicted drop shapes and viscosity maps for Newtonian and shear-thinning liquids when Re = 0.13, We = 0.000687, Fr = 0.00437. In that case Oh = 0.2. Shear-thinning parameters are $\lambda = 1$, $n = 0.2$, and $\eta_\infty = 0.2, 0.6$.

4   Conclusion

A volume-of-fluid numerical method has been used to predict the shape evolution of a drop of shear thinning liquid forming at a nozzle, directed vertically downwards in air. For a Newtonian drop, the shapes predicted closely match photographic images from a corresponding experiment. For shear thinning drops, the neck radius decreases more rapidly (that is, the approach to pinch-off is more rapid), and the final neck length is shorter, than for Newtonian drops with viscosity equal to the zero shear viscosity. The effect is qualitatively similar to reducing the viscosity of a Newtonian drop, and occurs because normal viscous stresses act to reduce the liquid pressure at the neck so that reducing the viscosity increases the pressure there and hence increases drainage out of the neck. Similar results have been predicted for the related problem of shear thinning liquid bridges [13].

References

[1] Y. Amarouchene, D. Bonn, J. Meunier and H. Kellay. Inhibition of the finite-time singularity during droplet fission of a polymeric fluid. *Phys. Rev. Lett,* 86(16):3558–3561, 2001.   C407

[2] B. Ambravaneswaran, E. D. Wilkes and O. A. Basaran. Drop formation from a capillary tube: Comparison of one-dimensional and two-dimensional analyses and occurrence of satellite drops. *Phys. Fluids,* 14(8):2606–2621, 2002.   C407

[3] Bird, R. B., Armstrong, R. C., and Hassager, O., *Dynamics of Polymeric Liquids*, Volume 1, 2nd edition, 1987, John Wiley & Sons, p. 171.   C410

[4] J. J. Cooper-White, J. E. Fagan, V. Tirtaatmadja, D. R. Lester and D. V. Boger. Drop formation dynamics of constant low viscosity, elastic fluids. *J. Non-Newt. Fluid Mech.,* 106(1):29–59, 2002. C406, C407

[5] J. Eggers. Nonlinear dynamics and breakup of free-surface flows. *Rev. Modern Phys.,* 69(3):865–929, 1997. C406

[6] D. Gueyffier, J. Li, A. Nadim, R. Scardovelli and S. Zaleski. Volume-of-fluid interface tracking with smoothed surface stress methods for three-dimensional flows. *J. Comp. Phys.,* 52:423–456, 1999. C407, C410

[7] D. M. Henderson, W. G. Pritchard and L. B. Smolka. On the pinch-off of a pendant drop of viscous fluid. *Phys. Fluids,* 9(11):3188–3200, 1997. C406

[8] J. Li and Y. Renardy. Numerical study of flows of two immiscible liquids at low Reynolds number. *SIAM Review,* 42(3):417–439, 2000. C410

[9] D. H. Peregrine, G. Shoker and A. Symon. The bifurcation of liquid bridges. *J. Fluid Mech.,* 212:25–39, 1990. C406

[10] M. Rudman. A volume tracking method for interfacial flows with large density variations. *Int. J. Numer. Meth. Fluids,* 28:357–378, 1998. C410

[11] R. M. S. M. Schulkes. The evolution and bifurcation of a pendant drop. *J. Fluid Mech.,* 278:83–100, 1994. C407

[12] E. D. Wilkes, S. D. Phillips and O. A. Basaran. Computational and experimental analysis of dynamics of drop formation. *Phys. Fluids,* 11(12):3577–3598, 1999. C406, C407, C414

[13] O. E. Yildirim and O. A. Basaran. Deformation and breakup of stretching bridges of Newtonian and shear-thinning liquids:

comparison of one- and two-dimensional models. *Chem. Eng. Sci.,* 56:211–233, 2001. C407, C414, C416

[14] D. F. Zhang, and H. A. Stone. Drop formation in viscous flows at a vertical tube. *Phys. Fluids,* 9(8):2234–2242, 1997. C407

[15] X. Zhang. Dynamics of growth and breakup of viscous pendant drops into air. *J. Colloid Interface Sci.,* 212:107–122, 1999. C407